J. Fluid Mech. (1974), *vol.* 63, *part* 1, *pp.* 1–20
Printed in Great Britain

An 'entraining plume' model of a spilling breaker

By M. S. LONGUET-HIGGINS AND J. S. TURNER
Department of Applied Mathematics and Theoretical Physics,
University of Cambridge

(Received 20 August 1973)

It is proposed that a spilling breaker can be regarded as a turbulent gravity current riding down the forward slope of a wave, and can be treated using methods which have been successful in other contexts. The whitecap retains its identity because it is lighter than the water below, owing to the trapping of air bubbles, and information from laboratory experiments is used to estimate the density of the air–water mixture in different circumstances. Entrainment of water from below, at a rate $E(Ri_0)$ which is a function of the overall Richardson number Ri_0, has two opposing effects. It provides increasing mass and buoyancy fluxes which can produce an accelerating flow and it also gives rise to a drag, because the entrained fluid has upslope momentum (in co-ordinates moving with the wave crest).

A similarity solution is obtained under the assumptions that the flow is steady in time, and that the slope and the density difference remain constant. In this solution, the thickness of the whitecap is proportional to the distance s measured from the crest of the wave. The tangential velocity is proportional to $s^{\frac{1}{2}}$. Since the velocity in a Stokes 120° angle is also proportional to $s^{\frac{1}{2}}$, this implies that such a flow can start from a small disturbance with zero flux, and propagate with constant acceleration. An important consequence of the analysis is that solutions of this kind are possible only when the slope and the density difference between the whitecap and the water below are sufficiently large; otherwise the upward drag dominates, and a self-sustaining flow cannot form. For a slope of 30°, near the crest of the breaking wave, the theory predicts that a density difference greater than 8% is required to sustain a steady motion, at which point the downslope velocity is 12% of the opposing velocity at the wave surface. A 'starting plume' model of the advancing front of the breaker is also discussed, which suggests that this too will be accelerating uniformly, but will have a velocity somewhat less than that in the flow behind.

A comparison with the laboratory observations of Kjeldsen & Olsen verifies several features of the model, including the order of magnitude of the relative velocities in the whitecaps and the wave beneath. It also reveals the intermittent nature of the flow, which is here explained as due to the intermittent rounding of the wave crest due to damping of the wave by the whitecap on the forward face.

1. Introduction

The physical importance of the phenomenon of wave breaking, both in shallow and in deep water, has been discussed in a recent review (Longuet-Higgins 1973*b*).

For example, it was pointed out that breaking waves are responsible for the conversion of wave momentum to surface currents, for the large-scale mixing of the surface layers of the ocean, and for enhancing the transfer of heat, salt and dissolved gases by the production of bubbles and spray.

Very little is known, however, about the mechanism of breaking of surface waves, especially in deep water. The form of the limiting wave has been calculated, following the early work of Stokes (1880), who showed that the steady progressive wave of maximum amplitude must have a sharp angle of 120° at the crest. It may be possible to follow the evolution of a wave up to the point of breaking by numerical methods similar to those used by Chan & Street (1970) for a wave in shallow water. However, apart from a study by Longuet-Higgins (1973*a*) (one feature of which will be discussed further below), no theoretical description has been given of the motion near the crest and in the resulting whitecap *after* the wave has broken. Mathematicians working in this field are accustomed to dealing with potential flows, and since the same methods cannot be applied to a turbulent breaker, this part of the problem tends to be neglected. In the present paper the turbulent character of the motion at this stage is taken as the starting-point, and ideas developed in another field are adapted to describe the progress of a whitecap down the front of a wave. Our theory is applied more particularly to breakers on a shelving beach, but there is nothing in the model which prevents it being applied also to deep-water waves.

The formulation of our model has been strongly influenced by laboratory studies of breaking waves and some associated phenomena. In particular Mason (1952) clearly distinguished two types of breaking wave: 'plunging breakers', in which the wave crest curls forward and plunges deeply into the slope of the wave some distance from the crest, and 'spilling breakers', in which the broken water seems to develop more gently from an instability at the sharp crest and forms a quasi-steady whitecap on the forward slope. Only this latter type, the spilling breaker, will be considered in the present paper. The contrast between these two types (and a third, the 'surging breaker' which can develop as a wave runs up on a steep beach) is shown very clearly in a recent ciné film made by Kjeldsen & Olsen (1971; see also Galvin 1972).

A characteristic property of a spilling breaker is that, as it breaks gently at the crest, it traps enough air bubbles for the resulting air–water mixture to be significantly lighter than the water below it. This density difference will inhibit mixing with the face of the wave, so that the whitecap rides on top of the sloping sea surface. The basic assumption of our theoretical model is that the whitecap can be regarded as a distinct turbulent flow, which is driven down the slope by the component of gravity in that direction in just the same way as a turbulent gravity current on a solid sloping boundary. As the flow continues, the turbulence will lead to the entrainment of water from the laminar wave surface below, and it will also result in the further incorporation of air, specially near the front of the whitecap, so that the density difference can be maintained.

The theory of Longuet-Higgins (1973*a*) suggests a model for the local flow near the forward edge of a spilling breaker, where the turbulent whitecap meets the undisturbed water surface. Here, on the contrary, we emphasize (in § 2) the

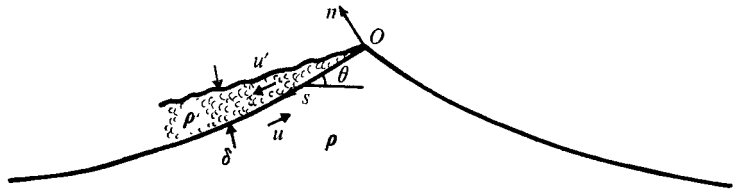

FIGURE 1. Sketch showing the features of a spilling breaker which are incorporated in the theoretical model. The wave is moving from right to left and has a whitecap on its forward face. The velocities in both the wave and whitecap are measured relative to the wave crest, with positive direction downwards.

properties of the flow some distance behind the front, using the balance of forces at a fixed cross-section in the manner proposed for turbulent gravity currents by Ellison & Turner (1959). Later (in § 6) it will be shown how the advance of the front can be described in a way which is consistent with this steady plume model. Common to both Longuet-Higgins's and Ellison & Turner's theories, however, is the assumption that there is a tangential stress at the boundary between the turbulent and laminar flows, due to the entrainment across this boundary

The several elements to be incorporated in the theory of § 2 are shown in figure 1. In co-ordinates moving with the phase velocity the flow at the surface of the waves is directed upwards towards the crest, with velocity decreasing to zero at the corner. On top of this is the whitecap, with gravity tending to drive it down the slope. Entrainment into this turbulent flow will add both water from below and air from above (or at the front). Mixing into the whitecap will be driven by turbulence produced by shear across the interface, but it will be inhibited by the fact that the turbulent air–water mixture in the whitecap is lighter than the water below which it entrains. The rate at which water is incorporated will depend on the velocity difference $u_0 = u' - u$ between the whitecap and the wave, on the density difference $\rho - \rho'$ (where ρ' is the mean density of the air–water mixture) and on the local length scale, say the depth δ. Following Ellison & Turner (1959) we suppose that the entrainment rate is a function of the overall Richardson number

$$Ri_0 = g'\delta \cos\theta / u_0^2, \tag{1}$$

where $g' = g(\rho - \rho')/\rho$ and θ is the slope. Rather less is known about the entrainment of air, but in § 3 we discuss laboratory measurements of air concentrations in hydraulic jumps (see, for example, Rajaratnam 1962) and in self-aerated flows on steep slopes (e.g. Straub & Anderson 1958) which allow us to put some limits on ρ'.

A similarity solution describing the development of the whitecap with distance from the crest is obtained in § 4. This must be an oversimplification of the actual unsteady flow, but it exhibits very clearly the most important physical features. The problem is unusual in that entrainment is both the driving and retarding mechanism: driving because it provides an increasing flux of water to accelerate the whitecap down the slope of the wave, and retarding because the

entrained water has momentum in the upslope direction. The balance between these opposing tendencies and gravity determines the behaviour of the spill, and it is shown in § 5 that only for large enough slopes and density differences can a downslope flow be formed. This problem has some features in common with the 'layer reversal' calculation of Ellison & Turner (1959). They showed how to calculate the strength of an opposing flow necessary to cause an inclined plume to reverse its natural direction of motion (with gravity) and to be swept along by the ambient stream.

In § 7 we make some comparisons between the results of the theory and laboratory measurements on spilling breakers, which confirm some of the features of our model but also reveal the intermittent character of the flow. This is discussed further in § 8, where a physical explanation is suggested.

2. The motion of an inclined plume entraining a varying ambient flow

The development of our model is adapted from that given by Ellison & Turner (1959), to which reference should be made for more details. Take the origin moving with the wave crest, the s axis along the wave slope, and the n axis perpendicular to this; the motion is assumed to be two-dimensional, i.e. independent of the distance along the crest. The mean velocity u' (positive in the downslope direction), depth δ and density ρ' in the whitecap at any s are defined using integrals of the local properties u'_n and ρ'_n across the flow:

$$u'\delta = \int_0^\infty u'_n dn, \tag{2}$$

$$u'^2\delta = \int_0^\infty u'^2_n dn, \tag{3}$$

$$u'\delta\rho' = \int_0^\infty u'_n \rho'_n dn. \tag{4}$$

There are certain differences between the present flow and the turbulent gravity currents considered previously which should be pointed out immediately. The density difference which drives the flow is now not the same as that which inhibits the entrainment. The full density difference between air and the air–water mixture in the breaker provides the driving buoyancy force, whereas it is the smaller density difference between the air–water mixture and the water below it which must be used when calculating entrainment. The entrainment assumption is summarized in the equation of continuity

$$d(\delta u')/ds = E|u_0|, \tag{5}$$

which states that the downslope mass flux is increased by entrainment at a rate proportional to the velocity difference between the whitecap and the wave slope below. The factor E is a function $E(Ri_0)$ of the overall Richardson number defined by (1), whose form is known from laboratory experiments. Implied by the use of Ri_0 as the only non-dimensional parameter involving the density difference is the Boussinesq approximation, which is used in all that follows.

In some cases where the proportion of air in the breaker is large, it may not be justifiable to neglect the variation of density in the inertia terms; but in view of the strong simplifications made in other ways it hardly seems appropriate to make the model too elaborate.

Another difference from the earlier theory becomes apparent in the derivation of the momentum equation. The velocity of the fluid being entrained into the breaker is not constant (as it was for the 'reversal' problem) but varies like $u \propto s^{\frac{1}{2}}$ (see § 4), and this introduces an extra term into the equation. It will also appear from the similarity solution that the plume velocity has this same dependence on s, so that the mass (or buoyancy) flux is increasing with distance. It is therefore not appropriate to seek solutions in which the buoyancy flux remains constant (as it does for a simple gravity current entraining ambient fluid which is at rest or in uniform motion). Instead, we shall suppose that the mean density ρ' of the air–water mixture remains substantially constant at all s, an assumption which will be shown in § 3 to have some experimental support.

The momentum equation, with an arbitrary exterior flow, can be written in the form

$$\frac{d}{ds}(u'^2\delta) = Euu_0 + S_2 g\delta \sin\theta - \tfrac{1}{2}S_1 \frac{d}{ds}(g\delta^2 \cos\theta), \tag{6}$$

where the Boussinesq approximation is used, and g rather than g' appears in the driving terms. On the left is the total rate of change of momentum flux. The first term on the right arises from the entrainment of fluid with velocity u at a rate Eu_0, the second represents the component of gravity accelerating fluid down the slope, and the last expresses the pressure force on the layer due to its changing depth, the pressure gradient being assumed quasi-hydrostatic, equal to $\rho' g \cos\theta$ normal to the surface. There is no solid boundary, and hence no other drag term. S_1 and S_2 are profile constants, which are required to allow for arbitrary density profiles. They are assumed to be independent of s and are defined as in Ellison & Turner (1959) by

$$S_1 \rho' \delta^2 = \int_0^\infty 2\rho'_n n \, dn \tag{7}$$

and

$$S_2 \rho' \delta = \int_0^\infty \rho'_n \, dn; \tag{8}$$

numerical estimates of them for air–water mixtures are given in § 3.

The term on the left of (6) and the first term on the right can be combined to give, for constant slope,

$$\frac{d}{ds}(\delta u' u_0) + \delta u' \frac{du}{ds} = S_2 g\delta \sin\theta - \tfrac{1}{2}S_1 \cos\theta \frac{d(g\delta^2)}{ds}, \tag{9}$$

which is the form used in the subsequent analysis. This differs from the momentum equation used by Ellison & Turner through the addition of the term in du/ds, which was zero in the previous application, where the external flow was uniform.

3. The processes of aeration

A detailed study of the mechanisms whereby air can be trapped and retained in a whitecap lies outside the scope of the present work. In order to proceed with the entraining plume model, however, we need to make some plausible assumption about the variation of ρ' with s and θ. In this section we must therefore digress briefly to discuss some relevant laboratory data on air entrainment in turbulent flows of water.

The first way in which air bubbles can be incorporated in the whitecap is by the over-running of a layer of air by the advancing front. This is similar to the trapping which occurs in the roller zone of hydraulic jumps, and which has been thoroughly studied experimentally (see the review by Rajaratnam 1967). According to Rajaratnam (1962), the concentration of air in the jump rises rapidly initially, then decreases gradually downstream. The air is fairly uniformly distributed vertically, and the maximum concentration depends systematically on the Froude number; it reaches values as high as 20 % over the range of conditions he studied. This suggests that the mean density ρ' in a vertical section can fall as low as $0{\cdot}8\,\mathrm{g/cm^3}$ near a vigorously turbulent front.

Another mechanism for the entrainment of air is the 'self-aeration' which can occur along the whole upper surface of a thin, vigorously turbulent flow (see, for example, Straub & Lamb 1956; Straub & Anderson 1958; Lakshmana Rao, Seetharamiah & Gangadharaiah 1970). High velocity open-channel flows (on a spillway, for instance) can begin to trap air when the turbulent boundary layer on the bottom reaches the surface, and 'white water' develops. The equilibrium distributions of air have been measured, and show a continuous variation from water containing a few air bubbles at the bottom to all air and no water at the top. Essentially there are two zones, the lower containing air bubbles suspended in water, and the upper consisting of water drops in air. An example of such a profile (converted to densities) and the associated velocity profile is shown in figure 2. Also of interest to us here is the observation that the mean concentration is a function mainly of the slope, with a weaker dependence on the Froude number. In figure 3 we summarize results of Straub & Anderson (1958) which show the variation with slope of the mean density over the whole depth, and that over the lower zone alone (the latter, shown in curve (a), being perhaps the more relevant for the present application). The dashed line represents a theoretical result which will be discussed in § 5.

Both these sets of observations suggest, therefore, that for whitecaps running down a given slope with (as will be shown) a constant Froude or Richardson number, it is appropriate to take the concentration of air, and hence the density, as constant. The air–water mixture is likely to be lighter on steep slopes (with ρ' as little as 0·7 near the crest of the wave where the slope is 30°) than it is lower down, but the effect of this will be investigated in our model by considering a series of fixed slopes and density differences, rather than a varying profile. Plots like figure 2 also allow us to estimate the values of S_1 and S_2 (from (7) and (8)) to use in the calculations, and we suggest $S_1 = 0{\cdot}80$ and $S_2 = 1{\cdot}00$ as representative values. The deviations of these constants from unity are measures

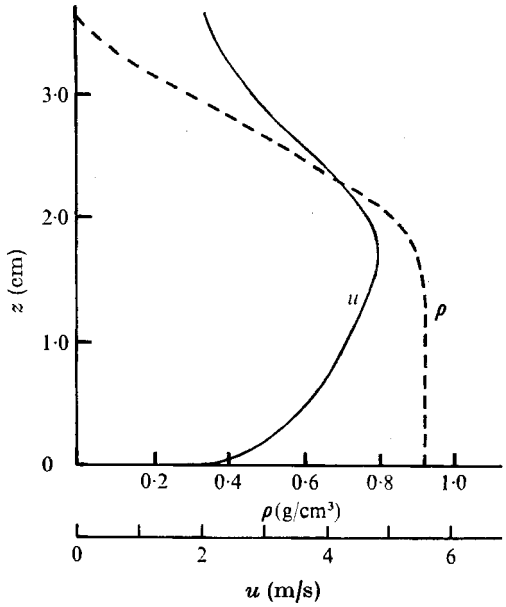

FIGURE 2. An example of the density and downslope velocity profiles measured through a self-aerated flow. (After Straub & Lamb 1956, figure 9.)

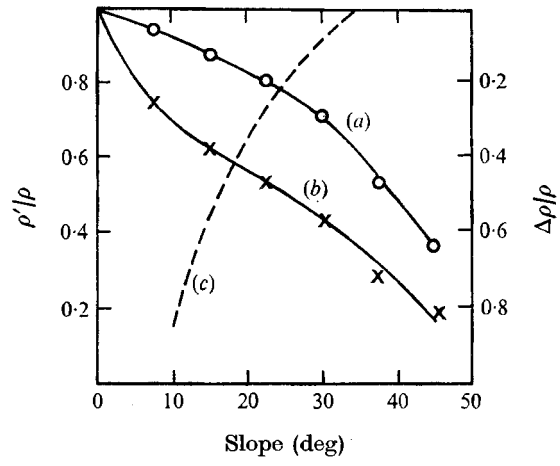

FIGURE 3. The mean density of self-aerated flows measured as a function of slope. (*a*) shows the result of averaging over a lower region consisting of air bubbles suspended in turbulent water, and (*b*) includes a more diffuse region of spray droplets above this. (After Straub & Anderson 1958, figure 6.) (*c*) represents our theoretical estimate of the minimum density differences required to produce a self-sustaining whitecap at various slopes.

of non-uniformity of the density distribution, and clearly constant density is a pretty good assumption; it is even better for the profiles measured in air-entraining hydraulic jumps.

There is another aspect of the self-aeration process which may have a bearing on whitecaps and should be mentioned now. As Gangadharaiah, Lakshmana Rao & Seetharamiah (1970) have pointed out, entrainment can occur only when the turbulence at the free surface has enough energy to overcome the surface-tension energy, and so allow eddies to project out of the surface and trap air bubbles. The criterion can be written, using an argument which will not be reproduced here, in the form

$$I = (\rho h \overline{U^2}/\sigma)(u_* h/\nu)^{\frac{1}{2}} > I_c, \tag{10}$$

where h is the depth, $\overline{U}$ the mean velocity, u_* the friction velocity, σ the surface tension and ν the kinematic viscosity. Thus the 'inception number' I must exceed some critical value I_c (of order 50 when the turbulent boundary layer has reached the surface) before air can be trapped at the surface in this way. For a breaker, this means that the flow must be deep enough and fast enough, or in terms of the theory in § 4 (which implies that $I \propto s^{\frac{1}{2}}$), must have progressed far enough from the crest, before this mechanism can operate. In the early stages of all breakers, over-running at the front will be the only way in which air is trapped, but it is possible that at a later stage whitecaps on large waves can be self-sustaining while those on small waves cannot.

4. Similarity solution for a spilling breaker

The boundary conditions and extra relations needed to simplify (5) and (9) and solve for δ and u' can now be written down. It will shortly be seen that the known velocity variation at the surface of the wave, together with the constant density difference suggested by the discussion in the previous section, leads to a simple similarity solution describing the progress of a spilling breaker.

It has already been pointed out that the surface velocity near the sharp crest varies like $u \propto s^{\frac{1}{2}}$; and if the slope below the crest is assumed to be constant, the same functional form will hold everywhere as a consequence of Bernoulli's equation. It is implied that the whitecap running down this slope remains thin, and does not itself substantially change the slope as it mixes with water from the wave. Since the pressure at the base of the turbulent layer is $g\rho'\delta\cos\theta$, the Bernoulli relation applied along this surface gives

$$\tfrac{1}{2}\rho u^2 = g\rho s\sin\theta - g\rho'\delta\cos\theta, \tag{11}$$

making the same quasi-hydrostatic assumption for the pressure as before. When the last term, which allows for the effect of the whitecap on the surface pressure, is neglected, then

$$u^2 = 2gs\sin\theta, \tag{11a}$$

and we obtain an explicit value for the constant of proportionality in the velocity relation.

It will be assumed that ρ' is constant, independent of s (though it can still be a function of θ). This suggests that $g' = g(\Delta\rho/\rho)$ should be taken as the second parameter (in addition to s) which is required to define the flow. It turns out to be more convenient to use s and g (not g') as scaling parameters, and to incorporate $\Delta\rho/\rho$ elsewhere in the analysis, but the assumption underlying this reduction should be kept in mind. Thus let us write

$$\delta = sk, \quad u = g^{\frac{1}{2}}s^{\frac{1}{2}}U, \quad u' = g^{\frac{1}{2}}s^{\frac{1}{2}}U', \tag{12}$$

where k, U and U' are dimensionless functions. (It is worth noting that these imply an 'eddy viscosity' proportional to $\delta u \propto g^{\frac{1}{2}}s^{\frac{3}{2}}$. Also if all velocities are proportional to one another, then the 'inception number' I defined by (10) behaves like $s^{\frac{1}{2}}$.)

Substituting (12) in (5) gives

$$d(g^{\frac{1}{2}}s^{\frac{3}{2}}kU')/ds = Eg^{\frac{1}{2}}s^{\frac{1}{2}}(U' - U)$$

or

$$k = \frac{2}{3}\left|\frac{U' - U}{U'}\right|E. \tag{13}$$

From the definition (1) we obtain

$$Ri_0 = \frac{g(\Delta\rho/\rho)\,ks\cos\theta}{(U' - U)^2 gs}$$

or

$$Ri_0 = \frac{2}{3}\left(\frac{\Delta\rho}{\rho}\right)\frac{E\cos\theta}{|U'(U' - U)|}. \tag{14}$$

Thus for particular values of U' and U (which specify the magnitudes of the velocities in the whitecap and in the fluid immediately below it), the turbulent layer thickens linearly with s, and the Richardson number remains constant. We are therefore dealing with a kind of 'normal' flow, whose gross properties can be described in the same terms at all s, in spite of the fact that the flow is accelerating uniformly down the slope. Note that the linear spread implies (from (11)) that the same form of velocity variation at the surface of the wave will hold even when the pressure effect of the whitecap is taken into account.

The momentum equation (9) becomes, using (12) and (13) and simplifying,

$$\frac{d}{ds}[U'(U' - U)\,gks^2] + kgs^{\frac{3}{2}}U'\frac{d}{ds}(s^{\frac{1}{2}}U) = S_2 gks\sin\theta - S_1 gk^2 s\cos\theta$$

or

$$U'^2(U' - U) + \tfrac{1}{4}U'^2 U = (\tfrac{1}{2}S_2\sin\theta)\,U' - \tfrac{1}{3}S_1(U' - U)\,E\cos\theta. \tag{15}$$

Equations (14) and (15), together with the empirical entrainment function $E(Ri_0)$, give three relations from which U', Ri_0 and E can be determined as functions of U. It is convenient to have an analytic expression for E, and the laboratory results of Ellison & Turner (1959) can in fact be represented to good accuracy by the form

$$E = \frac{0{\cdot}08 - 0{\cdot}1Ri_0}{1 + 5Ri_0}. \tag{16}$$

Calculations have been made for three slopes, 10°, 20° and 30°, and for three density differences at each slope. The values of the profile functions S_1 and S_2

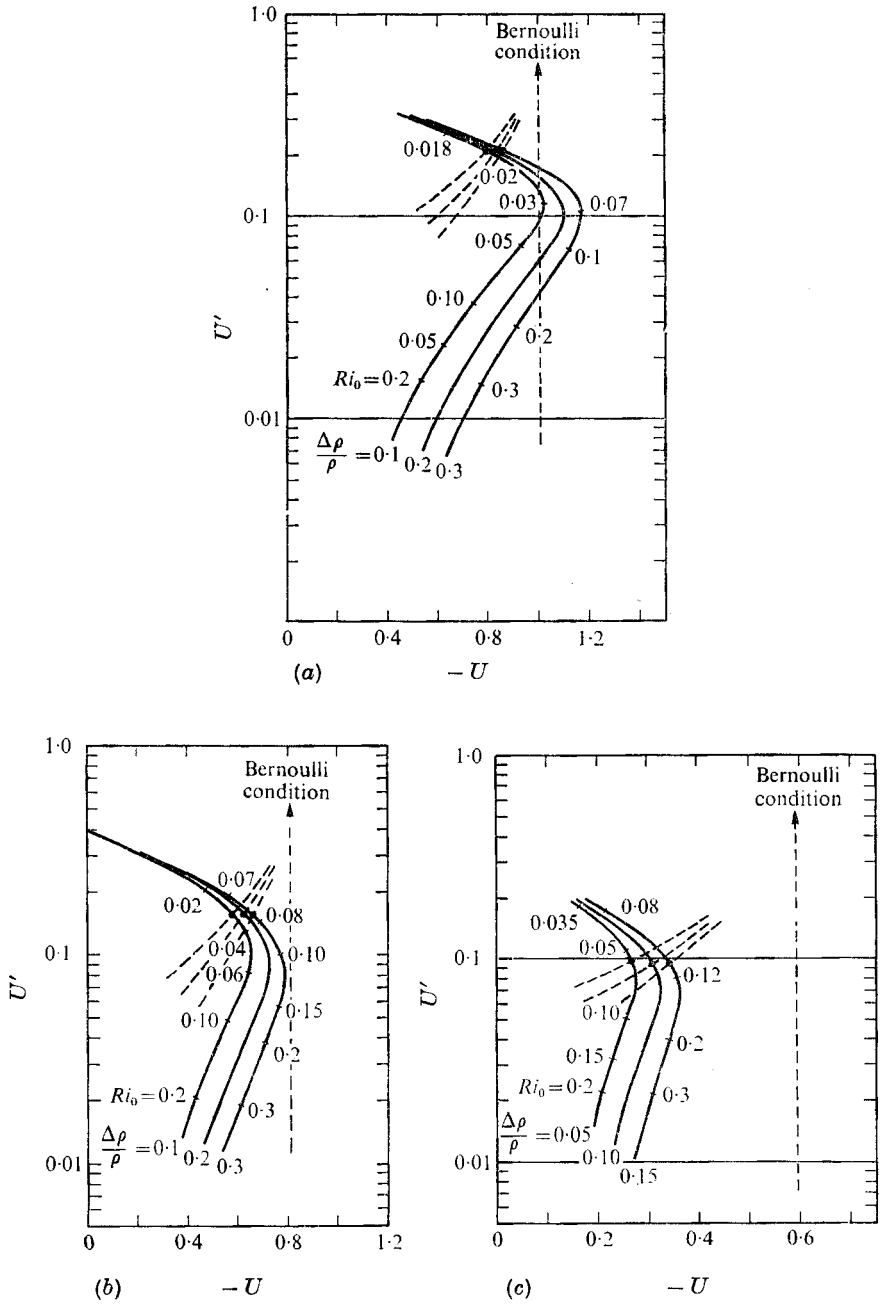

FIGURE 4. Non-dimensional whitecap velocity U' plotted against the upslope velocity U in the laminar flow below. (*a*) Slope of 30°. (*b*) Slope of 20°. (*c*) Slope of 10°. Plots for three density differences are given in each case; values of Ri_0 are marked on the curves. The vertical dashed line is drawn at the value of U obtained using the Bernoulli relation, and the inclined dashed lines show the modification due to the pressure effect of the whitecap.

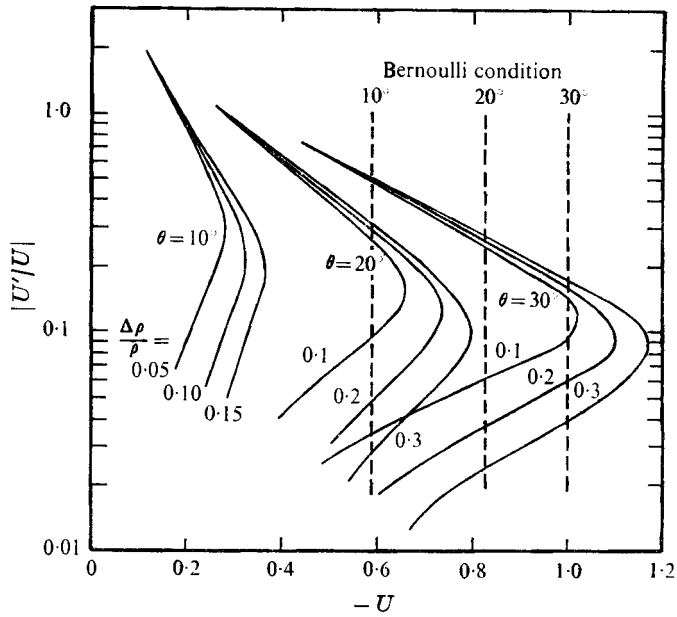

FIGURE 5. The ratio $U'/|U|$, as a function of U, for three slopes and several density differences, calculated from figure 4.

have been fixed at $S_1 = 0{\cdot}80$ and $S_2 = 1{\cdot}00$ throughout, as suggested in § 3. The solutions of interest are those for positive U' (appropriate for a whitecap going down the slope) as a function of U (negative, since the basic flow on the front surface of the wave is always upwards in co-ordinates moving with the crest). They have been found parametrically by fixing Ri_0, calculating E from (16) and then solving (14) and (15) for U and U'. The rate of spread can be found from (13), and used to evaluate the correction term in (11).

5. Results and discussion

The results of these calculations for a slope of 30° and $\Delta\rho/\rho = (0{\cdot}1, 0{\cdot}2, 0{\cdot}3)$ are shown in figure 4(*a*), where U' is plotted logarithmically against U on a linear scale, and values of Ri_0 are marked on the curves. The results for 20° and $\Delta\rho/\rho = (0{\cdot}1, 0{\cdot}2, 0{\cdot}3)$ are given in figure 4(*b*), and for 10° and $\Delta\rho/\rho = (0{\cdot}05, 0{\cdot}10, 0{\cdot}15)$ in figure 4(*c*) (note the changed scale of U in the latter figure). The corresponding values of U'/U for all nine calculations are plotted as functions of U in figure 5. The major features of interest occur in the range of parameters plotted.

The most important property of these curves is the maximum in $|U|$ as U' varies. This form implies that no solution for a downslope entraining flow, moving against the upslope velocity at the wave surface, is possible if $|U|$ is too large. But we already have an estimate of U (the non-dimensional velocity at the surface of the wave) in (11) or (11*a*); in the absence of a whitecap, which is the appropriate condition for the initiation process, this is just $(2\sin\theta)^{\frac{1}{2}}$. The corresponding values, $|U| = 1{\cdot}00$ at 30°, 0·83 at 20° and 0·59 at 10°, are shown as the

vertical lines on figures 4 and 5. The contrasts between these plots demonstrate clearly the effect of changes of slope and density difference, and sum up the main results of this paper. At a slope of 30° (near the crest of the wave) real solutions to the balance equations exist when $\Delta\rho/\rho$ is in the range suggested by experiment, and so a breaker can develop from a small disturbance and accelerate down the slope. The minimum density difference required at a slope of 30° is 8 %, well below the experimental values discussed in § 3.

The minimum density differences for other slopes are plotted as the dashed line on figure 3, for comparison with the experimental observations. At a slope of $34\frac{1}{2}°$, the development of a whitecap becomes possible, according to our theory, with zero density difference between the whitecap and the water below. As the slope decreases, larger and larger density differences are required to produce a self-sustaining flow, whereas the experimental curves on figure 3 show that the density difference will in fact be smaller at small slopes. Below a certain slope (between 18° and 24°, depending on the values we adopt for $\Delta\rho/\rho$) the upslope drag will dominate, and the whitecap can no longer propagate. This is consistent with the observation that an unsteady whitecap gets only part of the way down the face of the wave.

When the critical condition is passed, there are in general two solutions for the downslope velocity U' for the relevant value of $|U|$. The lower branch of the curves corresponds to larger Ri_0, low entrainment rates and much smaller downslope velocities. It can also be argued that this represents an unstable state, since the motion is dominated by gravity; a disturbance which increases the velocity difference between the laminar flow and the whitecap will lead to an increase in the mixing rate, larger velocities of the breaker, and a rapid transition to the upper branch. On the upper branch, however, extra mixing produces a substantial increase in the *drag*, which opposes the velocity fluctuation and restores the equilibrium. (A similar effect was noted by Ellison & Turner in their solution for flow reversal in a pipe.) At a slope of 30° the intersections of the physically relevant upper branches with $|U| = 1$ show that the whitecaps will have a downslope velocity which is much smaller than the upward velocity at the surface of the wave below. The ratio $U'/|U|$ ranges between 0·12 at $\Delta\rho/\rho = 0{\cdot}08$, the lower limit for the initiation of the flow, and 0·17 at $\Delta\rho/\rho = 0{\cdot}30$.

The variation of the angle of spread k (equation (13)) is also of interest, and this is plotted in figures 6 (*a*) and (*b*) for slopes of 30° and 10° as a function of U (both on linear scales). The corresponding values of Ri_0 are again marked on the curves. When Ri_0 is large k has its largest values in the range considered, which for $\theta = 30°$ at least are probably unrealistically high; but we should remember that these upper (dashed) parts of the curves correspond to the lower, unstable branches of figures 4 (*a*) and (*c*). As Ri_0 is decreased, so is k, and the values along the more relevant full parts of the curves seem physically much more reasonable.

With these estimates of k available, we can now calculate the effect of the whitecap on the velocity at the wave surface using (11). In the above discussion of the *marginal* state, it was appropriate to use (11*a*), since a whitecap cannot affect the wave before it has formed. Once this has happened, however, the opposing upslope velocity is reduced owing to the pressure effect of the whitecap,

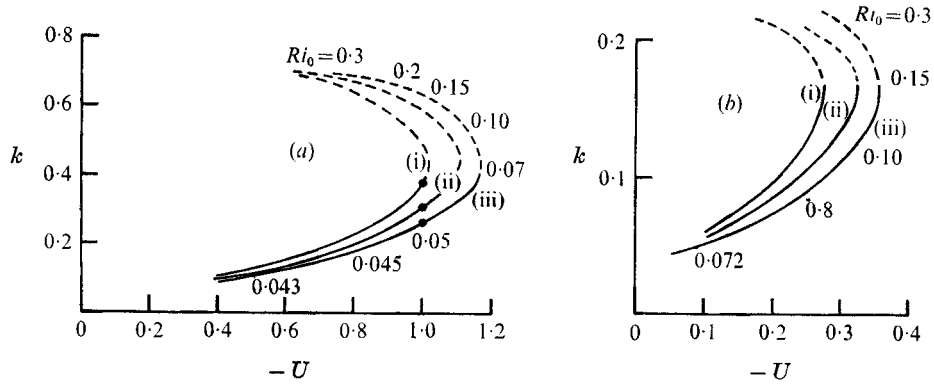

FIGURE 6. The angle of spread of whitecaps, calculated as functions of the dimensionless upslope velocity $U = u/(gs)^{\frac{1}{2}}$ for two slopes and various density differences. Values of Ri_0 are again marked on the curves. (*a*) Slope 30°: (i), (ii), (iii) correspond to $\Delta\rho/\rho$ = (0·1, 0·2, 0·3). (*b*) Slope 10°: (i), (ii), (iii) $\Delta\rho/\rho$ = (0·05, 0·10, 0·15).

which will be able to propagate more easily than it could initially. The values of the non-dimensional surface velocity $|U|$, corrected in this way, are plotted on figures 4(*a*), (*b*) and (*c*) at the values of U' derived in the earlier calculations. The crossing points (marked by bold dots) of these and the original curves thus represent possible solutions for a downslope flow, *including its effect on the velocity of the opposing flow which it is entraining*. On a slope of 30° (figure 4*a*) the effect is to increase the downslope velocity to 0·21 times the undisturbed surface velocity (this ratio depends very little on $\Delta\rho/\rho$). For 10° (figure 4*c*) the effect is more dramatic, since solutions now become possible where none existed before (with a downslope velocity 0·16 times that at the surface of the undisturbed wave). A possible implication is that a finite disturbance, due perhaps to a breaker spilling down from the higher slope above, may allow the flow to go further than would be expected from the argument based on the marginal stability of an undisturbed flow.

6. The motion of the front

We must now return to the question raised in the introduction: to what extent can a theory formulated for steady motion (i.e. assuming u and u' are independent of time at a fixed s) be used consistently to describe a flow which is certainly increasing in length as time goes on? We believe that this procedure can be justified, using an extension of the 'starting plume' model proposed by Turner (1962) for the axisymmetric plume and applied by Tsang (1970), among others, to the two-dimensional case.

This kind of model implies that the whole flow, the advancing front as well as the layer behind, will remain similar as it develops in time. First, it must be geometrically similar, so that the front also spreads linearly with distance (but perhaps at a different rate from the plume behind). Second, the power-law dependence of velocity on distance must be the same, with the front advancing

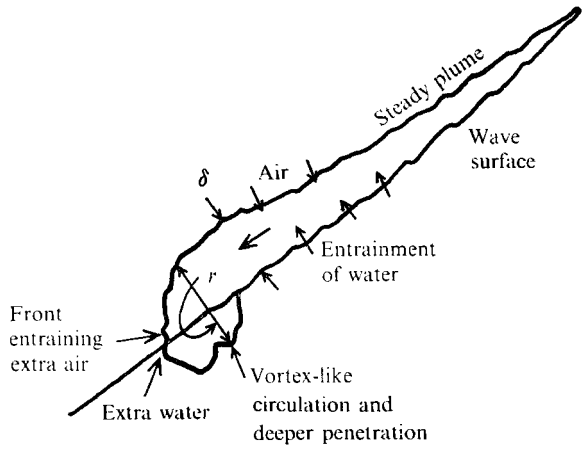

FIGURE 7. Sketch of the 'starting plume' interpretation of an advancing whitecap.

at some fraction of the layer velocity at the same position. The flow in the layer behind the front is just the same as that in a completely steady plume extending to infinity in the s direction (which has been implied in all the previous discussion). In a 'starting plume', however, this flow feeds momentum and buoyancy to the front at just the rate required to maintain similarity; but because of the accumulation of fluid at the front, the velocity of advance is reduced.

For both axisymmetric and two-dimensional starting plumes in neutral surroundings (i.e. with a constant buoyancy flux) the above picture has been shown to be consistent with the detailed equations of motion of the front. That is, if the region is regarded as a turbulent 'thermal', which is mixing with its surroundings and whose properties are also being changed by the injection of buoyant fluid from behind, then the deduced behaviour of the velocity and radius does indeed match that in the plume. What we must show now is that the same matching can be carried out for a two-dimensional plume whose properties are changing according to the similarity solution of § 4.

The model to be discussed is sketched in figure 7. The steady, established part of the whitecap is entraining water from below and air from above, at such a rate that the density of the air–water mixture remains constant. This also implies, according to the similarity solution, that the mass and buoyancy fluxes are increasing down the slope, with $\delta \propto s$ and $u' \propto g^{\frac{1}{2}}s^{\frac{1}{2}}$. Thus the whitecap is accelerating uniformly down the slope, and the position of a fluid particle as a function of time t is given by $s \propto t^2$. At the front the layer will feed fluid into a circulating region which is like one half of a vortex pair (cf. the two-dimensional starting plume). Extra entrainment of both air and water will certainly occur here, and the penetration of the surface of the wave below may well be greater than it is in the steady part of the flow.

The evidence from experiments on hydraulic jumps (§ 3) has suggested that the net effect will be to keep the density of the mixture near the front constant (at a given Froude number); in fact this result applies more particularly to the front, rather than to the flow behind. If we now assume that g' (or g) is the major

parameter determining the motion of the front, and seek a similarity solution, then again we find $u' \propto g^{\frac{1}{2}}s^{\frac{1}{2}}$. Thus the front and the layer behind it have the *same* velocity behaviour, essentially because constant acceleration is the only behaviour which is consistent with the use of g (or g') as a scaling parameter.

It may also be useful to sketch how this dimensional argument can be related to the dynamics of the front, regarded as a line vortex, though a description which is sufficiently detailed to include the different rates of spread and of advance must await more experimental information. Following Turner (1960) the impulse P per unit length of a vortex pair can be written in terms of the circulation K and the radius r as

$$P \propto Kr. \tag{17}$$

In the case of the similarity solution with constant acceleration this becomes

$$P \propto u's^2 \propto t^5, \tag{17a}$$

so that the rate of change of momentum is

$$dP/dt \propto t^4. \tag{18}$$

Contributing to this change of momentum is the downslope component of the total buoyancy per unit length of the front, which, assuming that $\Delta\rho$ remains constant, is

$$F \propto r^2 \propto t^4. \tag{19}$$

A second contribution comes from the flux of momentum from the layer behind

$$M \propto u'^2\delta \propto t^4. \tag{20}$$

Since (18), (19) and (20) have the same t dependence, the momentum equation expressing the balance between these terms will give a consistent description of the motion of the front.

The starting plume model, therefore, provides some justification for the kind of theoretical model we have used to describe a whitecap. If the similarity solution is a good approximation to the real, accelerating flow developing from a small disturbance at wave crest, then we would expect the front also to advance initially with constant acceleration. The velocity of the front could, however, be less than that predicted in figure 4.

7. Comparison with observation

We have compared our theoretical model with measurements taken from the recent film by Kjeldsen & Olsen (1971) of laboratory experiments on breaking waves. The measurements were made in a channel about 1 m wide and more than 10 m in length, and with rigid plane beaches of uniform gradient. In the sequences on spilling breakers the waves had generally the appearance of solitary waves. We analysed two such sequences in detail, and the conclusions being similar in the two cases, only one will be presented here.

We measured, frame-by-frame, the following parameters:

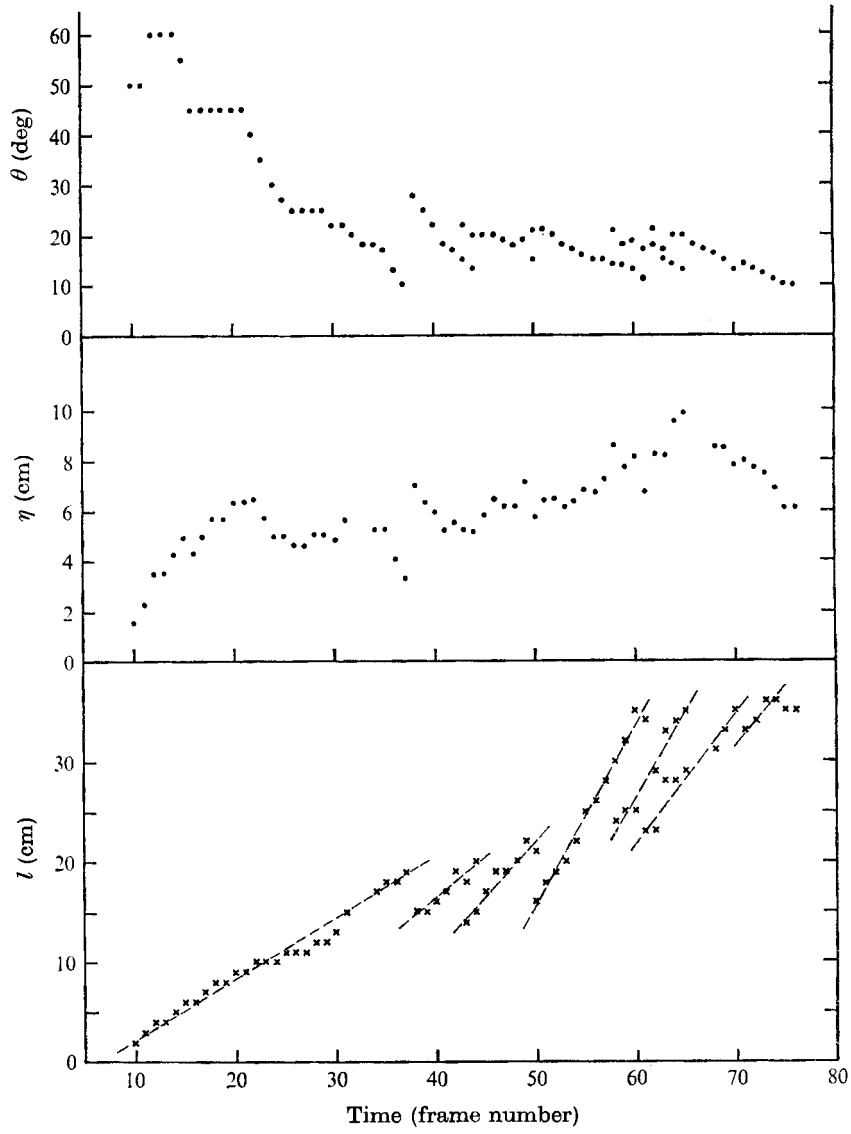

FIGURE 8. Measurements of the properties l, η and θ of a whitecap (as defined in the text), taken from a spilling breaker sequence in the film by Kjeldsen & Olsen. Note the intermittent nature of the flow.

X = the horizontal distance of the wave crest (identified by its maximum curvature) relative to a fixed mark in the wave tank.

H = the height of the wave crest above the bottom.

l = the distance from the crest to the 'toe' of the whitecap, measured along the surface of the wave.

θ = the inclination to the horizontal of the line joining the crest to the 'toe' of the whitecap.

From these we calculated the horizontal and vertical distances (ξ and η) of

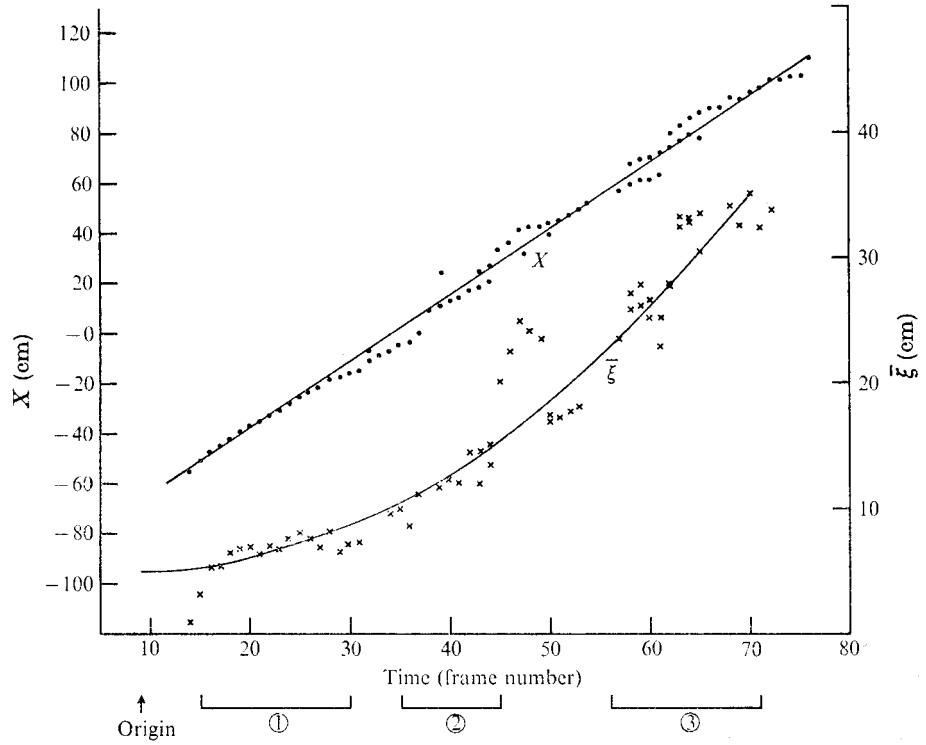

FIGURE 9. The measured horizontal position of the crest X, and the horizontal distance ξ between the toe of the whitecap and the smoothed position of the crest, plotted for the same film sequence as figure 8. The time intervals marked along the bottom are those used to obtain the average values given in the table.

the toe relative to the wave crest. We also measured the maximum thickness δ of whitecap on each frame, and occasionally the angle of the wedge, approximately δ/l.

In figure 8 are plotted the quantities l, θ and $\eta = l\sin\theta$, as functions of the frame number. It can be seen at once that, apart from a general increase in l and η with time, there is also a marked intermittency. The observations showed that after initiation of the whitecap there was a preliminary period of growth, after which the wave crest would become more rounded. A part of the whitecap would then be dragged over the crest, which then became sharp again. The reasons for this behaviour are discussed in § 8. Sometimes two wave 'crests' could be identified on a single frame and in this case the measurements of both are plotted.

However, most of the intermittency in l shown in figure 8 is due to the oscillation in the horizontal position of the crest, not the toe. This is shown in figure 9, where we have plotted the horizontal co-ordinate $\bar{\xi}$ of the toe relative to the *smoothed* position of the crest. It will be seen that, after an initial jump, $\bar{\xi}$ increases much more smoothly than ξ (note the change in scale). A parabola, representing a uniform acceleration, can be drawn to fit the points reasonably

well, apart from a brief excursion in the middle, associated with a transient increase in the rate of advance of the crest.

The corresponding velocities can be estimated in the absence of any precise record of the film speed used by Kjeldsen & Olsen, and using only the fact that the mean phase velocity $d\bar{X}/dt$ is given accurately for a solitary wave by Scott Russell's formula $(gH)^{\frac{1}{2}}$. According to our model u may be taken as $(2g\eta)^{\frac{1}{2}}$ very nearly, where η is the measured vertical distance from the crest. The smoothed downslope velocity $d\bar{l}/dt = \sec\theta(d\bar{\xi}/dt)$ can be found from the parabola fitted to the points in figure 9, and compared with $d\bar{X}/dt$ from that same plot. Denoting the ratio $(d\bar{\xi}/dt)/(d\bar{X}/dt)$ by R say, we obtain finally

$$(d\bar{l}/dt)/u = R\sec\theta(H/2\eta)^{\frac{1}{2}}. \tag{21}$$

The results of this calculation at three times during the run are shown in the table. H, η and θ were evaluated locally, using averages of 10–15 values centred on the time of interest. This procedure is not quite consistent with the fitting of a line of constant slope over the whole range of X, but it is sufficiently accurate for the present purpose. In the early stages, immediately after the initiation of the whitecap, its behaviour is well described by the theory; it is accelerating down the slope, and moving with 16% of the upslope velocity in the wave underneath it. At later times, however, its velocity is an increasing fraction of u. This could be a consequence of two effects. First, there is the influence of the whitecap on the velocity of the upslope flow beneath it (which has been described in the earlier theoretical sections). Second, the change in slope with time leads to a decrease in the deduced value of η, an effect which is not included in the simple theory, but which is discussed further below.

Interval	t (frames from initiation of spill)	R	θ	H (cm)	η (cm)	$(d\bar{l}/dt)/u$
1	13	0·078	35°	29·7	5·3	0·16
2	31	0·187	21·5°	27·8	5·8	0·31
3	54	0·326	17·5°	24·6	8·2	0·42

TABLE 1. Summarizing the mean properties of a spilling breaker as measured from the film at three times after the initiation of a whitecap.

8. The energy balance of the waves

We shall now give an interpretation of the intermittency seen in figures 8 and 9.

A rough estimate of the energy lost through breaking may be made as follows. If we consider the whitecap as a mass of lighter fluid resting inertly on the forward face of the wave, the weight W of the whitecap must do work against the wave at a rate $Wv\cos\theta$, where v is the normal velocity at the interface and θ is the angle between the normal and the vertical. Since $v = c\sin\theta$, the rate of working is $cW\cos\theta\sin\theta$ and the total work done during one wave period is $WL\cos\theta\sin\theta$,

where L is the wavelength. This must be equal to the difference in the integrated flux of energy across the two ends of a horizontal interval of length L. (We ignore the loss of kinetic energy through entrainment into the wedge, which can be shown to be relatively small.) Now the integrated energy flux is simply the total energy of the wave, which for a solitary wave of maximum amplitude in water of uniform depth is equal to $\gamma\rho g h^3$, where h is the undisturbed depth and γ is a factor equal to about 1·0 (see Longuet-Higgins 1974). However, in shoaling water γ may be of order 5 or more (see Ippen & Kulin 1955). We have then

$$WL\cos\theta\sin\theta = -Ld(\gamma\rho g h^3)/dX. \tag{22}$$

But also

$$W = \tfrac{1}{2}\rho' g l^2 \sin\alpha, \tag{23}$$

where l is the length of the whitecap and α the angle of the 'wedge'. From these two equations we obtain

$$(l/h)^2 = \frac{12\gamma(\rho/\rho')\,|dh/dX|}{\sin 2\theta \sin\alpha}. \tag{24}$$

Substituting the typical values

$$\rho/\rho' = 1{\cdot}2, \quad |dh/dX| = 0{\cdot}03, \quad \alpha = 20°, \quad \theta = 30°, \quad \gamma = 3{\cdot}0,$$

we find $l/h = 1{\cdot}7$. The total depth H (on beaches of this slope) being about $2{\cdot}6h$, we have

$$l/H \doteq 0{\cdot}65. \tag{25}$$

We conclude that for a solitary wave to lose energy gradually to a spilling breaker, the length l of the whitecap should be a certain fraction, about half, of the total height of the wave.

However, we have already shown that there is a tendency for the length of the whitecap to increase and for the whitecap to spread down the forward face of the wave, whereas on a shelving beach H tends constantly to diminish. It follows that a steady state cannot normally be achieved. The whitecap can therefore exist only intermittently.

From the observations it appears that what actually occurs in a spilling breaker is that, as the whitecap grows, the rate of damping described above overtakes the effect of wave steepening due to shoaling. The wave crest then becomes rounded. This reduces the slope, and enables part of the whitecap to be dragged over the crest. The wave can then steepen again, and the whitecap resumes its growth. The process is repeated, until the wave energy is no longer sufficient to maintain it.

9. Conclusion

We have shown how several features of a spilling breaker can be described using a model which regards the whitecap as a turbulent plume, running down the forward slope of the wave and entraining the laminar fluid below it. In particular, the predicted sensitive dependence on the slope, and the magnitude of the downslope velocity, are in agreement with laboratory observations of spilling breakers.

Our explicit similarity solutions, however, are based on the assumption of

constant density of the air–water mixture in the whitecap. While this has some support from the limited observations of air-entraining flows of other kinds, it is the weakest point of our present model, and further work on this aspect of the problem would be desirable. It seems probable that the spreading of a whitecap down the forward face of a wave is sometimes limited not by the surface slope, but by the decrease of the density difference due to the loss of air bubbles as they rise through the whitecap. A fully time- and space-dependent description of the concentration of air in a whitecap should be our eventual aim. Nevertheless, the balance of forces we have used in this paper will still be relevant in any theory which takes the turbulence in whitecaps properly into account.

One of us (J.S.T.) acknowledges the support of a grant from the British Admiralty.

REFERENCES

CHAN, R. K. C. & STREET, R. L. 1970 Shoaling of finite amplitude waves on plane beaches. *Proc. 12th Conf. on Coastal Engng*, pp. 345–362. New York: A.S.C.E.

ELLISON, T. H. & TURNER, J. S. 1959 Turbulent entrainment in stratified flows. *J. Fluid Mech.* **6**, 423–48.

GALVIN, C. J. 1972 Wave breaking in shallow water. In *Waves on Beaches* (ed. R. E. Meyer), pp. 413–456. Academic.

GANGADHARAIAH, T., LAKSHMANA RAO, N. S. & SEETHARAMIAH, K. 1970 Inception and entrainment in self-aerated flows. *J. Hyd. Div. A.S.C.E.* HY **7**, 1549–1565.

IPPEN, A. T. & KULIN, G. 1955 Shoaling and breaking characteristics of the solitary wave. *M.I.T. Hydrodynamics Lab. Tech. Rep.* no. 15.

KJELDSEN, S. P. & OLSEN, G. B. 1971 Breaking waves (16 mm film). Technical University of Denmark, Copenhagen.

LAKSHMANA RAO, N. S., SEETHARAMIAH, K. & GANGADHARAIAH, T. 1970 Characteristics of self-aerated flows. *J. Hyd. Div. A.S.C.E.* HY **2**, 331–355.

LONGUET-HIGGINS, M. S. 1973*a* A model of flow separation at a free surface. *J. Fluid Mech.* **57**, 129–148.

LONGUET-HIGGINS, M. S. 1973*b* The sea surface. Review lecture to Royal Society of London, 5 April 1973.

LONGUET-HIGGINS, M. S. 1974 On the mass, momentum, energy and circulation of a solitary wave. *Proc. Roy. Soc.* A. In the Press.

MASON, M. A. 1952 Some observations of breaking waves. In *Gravity Waves*, pp. 215–220. U.S. Nat. Bur. Standards. Circular no. 521.

RAJARATNAM, N. 1962 An experimental study of the air entrainment characteristics of hydraulic jump. *J. Inst. Engng India*, **42**, 247–273.

RAJARATNAM, N. 1967 Hydraulic jumps. *Advances in Hydroscience*, vol. 4, pp. 197–280. Academic.

STOKES, G. G. 1880 On the theory of oscillatory waves. *Math. & Phys. Papers*, **1**, 197–229, 314. Cambridge University Press.

STRAUB, L. G. & ANDERSON, A. G. 1958 Experiments on self-aerated flow in open channels. *J. Hyd. Div. A.S.C.E.* HY **7**, 1–35.

STRAUB, L. G. & LAMB, O. P. 1956 Studies of air entrainment in open-channel flows. *Trans. A.S.C.E.* **121**, 30–44.

TSANG, G. 1970 Laboratory study of two-dimensional starting plumes. *Atmos. Envir.* **4**, 519–544.

TURNER, J. S. 1960 A comparison between buoyant vortex rings and vortex pairs. *J. Fluid Mech.* **7**, 419–432.

TURNER, J. S. 1962 The starting plume in neutral surroundings. *J. Fluid Mech.* **13**, 356–368.